Biomedicine & Pharmacotherapy 131 (2020) 110669

Contents lists available at ScienceDirect

Biomedicine & Pharmacotherapy

journal homepage: www.elsevier.com/locate/biopha

Berberine alleviates type 2 diabetic symptoms by altering gut microbiota and reducing aromatic amino acids

Ye Yao [a,b], Han Chen [a,b], Lijing Yan [a,b], Wenbo Wang [a,b], Dongsheng Wang [a,b,*]

[a] Institute of Integrated Traditional Chinese and Western Medicine, Xiangya Hospital, Central South University, Changsha, 410008, China
[b] Hunan Key Laboratory of Traditional Chinese Medicine for Gan of State Administration, Central South University, Changsha, 410008, China

ARTICLE INFO

Keywords:
Berberine
Gut microbiota
16S rRNA gene sequencing
Metabolomics
AAAs
T2DM

ABSTRACT

Objective: Berberine (BBR), which is extracted from traditional Chinese herb, is abundant in *Coptis chinensis* and *Berberis vulgaris*, with a treatment on type 2 diabetes mellitus (T2DM). However, its oral bioavailability is poor. Therefore, the ability of BBR to regulate gut microbiota and intestinal metabolites might exist. This study aimed to investigate changes in gut microbiota and intestinal metabolites, and to reveal the potential mechanism of BBR.

Methods: To observe the role of gut microbiota in the treatment of T2DM by BBR, antibiotics intervened gut microbiota was used in this study, and the therapeutic effects of BBR were evaluated. A 16S rRNA gene sequencing approach was utilized to analyze gut microbiota alterations, and UHPLC-QTOF/MS-based untargeted metabolomics analysis of colon contents was used to identity differential intestinal metabolites. Finally, serum aromatic amino acids (AAAs) were absolutely quantified using LC/MS.

Results: Inhibition of the blood glucose levels, and improvements in glucose tolerance and serum lipid parameters were observed in the BBR treated group. Type 2 diabetic symptoms in rats in the BA group (treated with antibotics and BBR) were alleviated. However, the therapeutical effects are weaker in the BA group compared with the BBR group, indicating that BBR can be used to treat type 2 diabetic rats immediately, and modulation of gut microbiota is related to the mechanism of BBR in the treatment of T2DM. The community richness and diversity of the gut microbiota were significantly increased by BBR, and the relative abundance of *Bacteroidetes* was increased in the BBR group, which was accompanied by a decreased relative abundance of *Proteobacteria* and *Verrucomicrobia* at the phylum level. At the family level, a probiotic *Lactobacillaceae* was significantly upregulated not only in the BBR group but also in the BA group and was negatively associated with the risk of T2DM. Metabolomic analysis of colon contents identified 55 differential intestinal metabolites between the BBR group and the model group. AAAs, including tyrosine, tryptophan and phenylalanine, were obviously decreased in the BBR group not only in the colon contents but also in the serum.

Conclusions: These results demonstrated that BBR could alleviate symptoms in type 2 diabetic rats by affecting gut microbiota composition and reducing the concentration of AAAs.

Abbreviations: AAAs, Aromatic amino acids; AUC, area under the curve; BBR, berberine; BCAAs, branched-chain amino acids; COG, clusters of orthologous groups of proteins; ESI, electrospray ionization; FBG, fasting blood glucose; FC, fold change; HOMA-IR, homeostasis model assessment of insulin resistance index; HDL-C, high-density lipoprotein cholesterol; IDA, information dependent acquisition; UHPLC-QTOF/MS, Ultra high performance liquid chromatography coupled with quadrupole-time-of-flight tandem mass spectrometry; LDL-C, low-density lipoprotein cholesterol; LEfSe, Linear discriminant analysis effect size; OGTT, blood glucose levels of the oral glucose tolerance test; OTC, over-the-counter; OTUs, operational taxonomic units; OPLS-DA, orthogonal partial least-squared discriminant analysis; PCoA, principal coordinate analysis; QC, quality control; TMAO, trimethylamine-*N*-oxide; TC, total cholesterol; TG, Triglyceride; STZ, streptozocin; SCFAs, short-chain fatty acids; VIP, variable importance in the projection.

* Corresponding author at: Institute of Integrated Traditional Chinese and Western Medicine, Xiangya Hospital, Central South University, Changsha, 410008, China.

E-mail addresses: xyyaoye@csu.edu.cn (Y. Yao), xyhanchen@aliyun.com (H. Chen), xylijingyan@163.com (L. Yan), wangwenbo@csu.edu.cn (W. Wang), wdsh666@126.com (D. Wang).

https://doi.org/10.1016/j.biopha.2020.110669
Received 23 May 2020; Received in revised form 14 August 2020; Accepted 20 August 2020
Available online 13 September 2020
0753-3322/© 2020 The Authors. Published by Elsevier Masson SAS. This is an open access article under the CC BY-NC-ND license (http://creativecommons.org/licenses/by-nc-nd/4.0/).

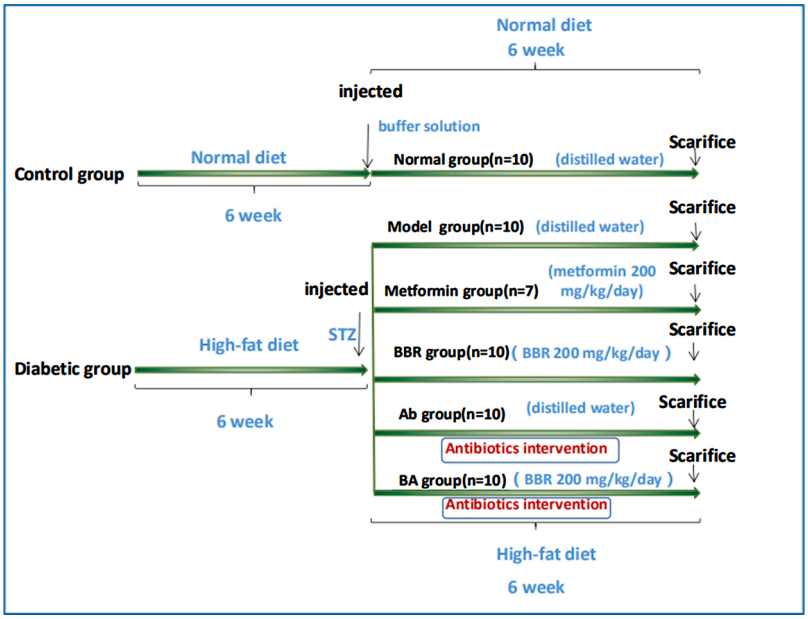


Fig. 1. Animal experimental design.

1. Introduction

Type 2 diabetes mellitus (T2DM) is characterized by hyperglycemia, which is one of the most common chronic diseases. Its incidence rate increases steadily together with the improvement of living level and population aging, which represents an increasing burden to medical services [1]. Oral drugs and insulin supplement are the current main treatment of T2DM, but some side effects, such as liver problems, and lactic acidosis, are noted [2]. Therefore, a continuous search for alternative drugs and natural medicines for T2DM with high efficiency and low toxicity is necessary.

Berberine (BBR) is an isoquinoline quaternary alkaloid that is extracted from Chinese traditional medicine and widely exists in *Coptidis rhizoma* and *Berberis vulgaris* [3,4]. BBR and berberis plants have a long history of treating disease in both western and Chinese traditional medicine [5]. In China, BBR has been used as an over-the-counter (OTC) drug for decades to treat bacteria-caused diarrhea, and vast experimental evidences have revealed its anti-inflammatory and anti-tumor effects as well as its ability to reduce blood glucose and cholesterol [6–10].

A growing number of studies have shown the associations between gut microbiota dysbiosis and diabetes, suggesting gut microbiota as a potential drug target [11,12]. Gut metabolites, which are produced by gut microbiota, such as trimethylamine-*N*-oxide (TMAO), short-chain fatty acids (SCFAs), branched-chain amino acids (BCAAs), bile acids, vitamins and aromatic amino acids (AAAs) were reported to be involved in T2DM. Among them, SCFAs are beneficial for the treatment of diabetes, and TMAO and BCAAs are risk factors for diabetes [13–18]. AAAs, including tyrosine, tryptophan and phenylalanine are derived from the diet and vital for normal growth and function at the cell and organism levels [19]. Many studies have found that increased AAA concentrations are associated with an increased risk of T2DM [19–22]. A randomized trial found that metformin could decrease the concentration of tyrosine and phenylalanine, indicating that reducing levels of AAAs could alleviate type 2 diabetic symptoms [21].

BBR is useful for the treatment of diabetes as demonstrated by a wealth of results from randomized controlled clinical trials [23]. Many studies seek to reveal the anti-diabetic mechanism of berberine [24]. Some studies found that BBR could alter glucose metabolism through the stimulation of glycolysis by increasing glucokinase activity and insulin secretion and suppressing hepatic gluconeogenesis and adipogenesis, and 5′-adenosine monophosphate kinase (AMPK) activation is important for these effects [24–26]. On the other hand, some studies found that BBR alleviated diabetic symptoms via antioxidation effects [24,27–29]. However, the direct mechanism of BBR's anti-diabetic properties is not completely understood.

Although BBR is useful for T2DM, the oral bioavailability of BBR is poor, at less than 1.0 % [30]. Therefore, BBR may act via possible mechanisms of regulating gut microbiota and intestinal metabolites to produce therapeutic effects. As is well known, numerous metabolites are present in the intestinal tract, many of which are related to gut microbiota. In this study, we aimed to reveal the impact of BBR in type 2 diabetic rats, especially modulation of gut microbiota and intestinal metabolites. We implemented 16S rRNA gene sequencing on the MiSeq platform to analyze the changes in gut microbiota after oral administration of BBR. Furthermore, a UHPLC-QTOF/MS-based untargeted metabolomics analysis of colon contents was performed to reveal alterations in gut metabolites, and to obtain a better understanding of the impacts of BBR on type 2 diabetic rats.

2. Materials and methods

2.1. Reagents and diet

BBR, metformin, vancomycin, neomycin and metronidazole were obtained from Shanghai Yuanye Bio-TechnologyCo., Ltd (source: Shanghai, China). Streptozotocin (STZ), tyrosine, tryptophan and phenylalanine were purchased from Sigma-Aldrich Co., Ltd. (source: St. Louis, MO, USA). Citric acid and sodium citrate were purchased from Sinopharm Chemical Reagent Co., Ltd. (source: Shanghai, China). BBR and metformin were dissolved in distilled water before being intragastrically administered. STZ was dissolved in sodium citrate-citric acid buffer (10 mg/mL, pH = 4.5).

A high-fat diet was obtained from Beijing Ke-ao-xie-li Feed Co., Ltd. (Beijing, China). The high-fat diet included the following: 68.75 % normal diet (nutritional ingredients was tabled in **Table S1**),10 % sucrose, 10 % lard, 0.25 % bile salt, 1% cholesterol and 10 % yolk powder.

2.2. Animal experiments

Sixty male Sprague-Dawley (SD) rats (weighing 220 ± 20 g) were purchased from the Department of Experimental Animals, Central South

NNB Exh. 2084, p. 002

Table 1
Standard curves of AAAs.

Component Name	Mass Information	Retention Time	Linear	R^2
Tyrosine	182.1 / 136.1	7.827435668	y = 0.03426 x + 0.05444	0.99915
Tryptophan	205.1 / 146.3	5.723980794	y = 14.86904 x -6.45132	0.99822
Phenylalanine	166.1 / 103.1	5.039311654	y = 0.19092 x + 0.14375	0.99984

University (Changsha, China, batch number: 43004700048115, permission code: SCXK2016−0002). The rats were raised in a group of 3 rats per cage with the relative humidity at 50 ± 15 %, a temperature of 25 ± 2 °C, and a 12 -h dark-light cycle with sterile water and diet. This animal experiment was approved by the Institutional Animal Care and Use Committee of Central South University (Changsha, China, permit number:2019sydw0169).

After 1 week of acclimatization, 60 rats were randomly stratified into 2 groups: a control group (n = 10) fed a normal diet and a diabetic group (n = 50) fed a high-fat diet. After being fed a high-fat diet for 6 weeks, each of the 50 rats fasted for 8 h and was injected intraperitoneally with STZ (35 mg/kg) [31]. Each of the control group rats was injected with an equivalent sodium citrate-citric acid buffer vehicle. Three days later, FBG (fasting 8 h) was measured with a glucometer (Accu-Chek (R) Active, Roche Diagnostics GmbH, Mannheim, Germany) by tail vein sampling. The rats with an FBG ≥ 16.7 mol/L for 3 days were considered as diabetic rats [31,32]. Finally, all the 47 rats met the above criteria and were once again randomly stratified into 5 groups: 1) the model group (n = 10), 2) the metformin group (n = 7), 3) the BBR group (n = 10), 4) the antibiotics group (Ab group, n = 10), and 5) the antibiotics + BBR group (BA group, n = 10). The above 5 groups were fed a high-fat diet continuously for 6 weeks until the end of the study.

In addition, the BBR group and the BA group were treated daily with the corresponding dose of BBR (200 mg/kg/day) by intragastric administration [10,15,33]. The metformin group received 200 mg metformin/kg/day [18,32]. The normal group, the model group and the Ab group were given an equal volume of distilled water by intragastric administration at the same time. The Ab group and BA group were treated with 100 μg/mL metronidazole, 25 μg/mL vancomycin and 50 μg/mL neomycin in sterile water per day [34]. The pharmacological interventions were sustained for 6 weeks, and FBG was recorded every week (Fig. 1).

2.3. Sample collection

At the end of the trial, the rats were fasted for 8 h and were anesthetized by inhaled isoflurane (concentration maintained at approximately 2%, Shanghai Abbott Laboratories, Shanghai, China). Ultimately, the rats were sacrificed after blood collection through the heart. The serum was obtained following centrifugation at 3500 rpm (4 °C) for 15 min. Colon contents were obtained after opening the abdominal cavity, and were stored in 2 mL cryotubes. The samples of serum and colon contents were stored at −80 °C for further analysis. All the experimental materials were sterile.

2.4. Oral glucose tolerance test

An oral glucose tolerance test (OGTT) was performed at the end of the trial. All rats were fasted 8 h and were given D-glucose (2.0 g/kg, 25 % solution) by intragastric administration. Blood glucose was determined with a glucometer by tail vein sampling at 0 min, 5 min, 10 min, 30 min, 60 min and 120 min. The area under the curve (AUC) was calculated with every blood glucose level (BGL) multiplied by time

$$AUC = BGL_1 *0 + BGL_2*5 + BGL_3*10 + BGL_4*30 + BGL_5*60 + BGL_6*120.$$

2.5. Biochemical assays

The serum levels of total cholesterol (TC), triglyceride (TG), high-density lipoprotein cholesterol (HDL-C), low-density lipoprotein cholesterol (LDL-C), and serum glucose were determined immediately using an automatic biochemical analyzer (SS00PP, Secomam, France). The level of fasting serum insulin was quantified using an ELISA kit (EZRMI-13 K, Merck Millipore Co., Ltd, Darmstadt, Germany), and all the steps strictly complied with the manufacturer's instructions. HOMA-IR was calculated with the following formula:

HOMA-IR = serum glucose levels(mmol/l) * insulin levels(mU/l) / 22.5

2.6. Bacterial composition analysis

Initially, the samples of colon contents were thawed at 4 °C. We used a TIANmap Stool DNA Kit (DP328, TIAGEN biotech Co., Ltd., Beijing, China) to extract genomic DNA, and all the processes followed the manufacturer's instructions. The quantity of DNA was confirmed with a Nanodrop device (NC2000, Thermo Scientific), and the quality was tested by agarose gel electrophoresis. The microbiota V3-V4 regions (338F-806R) of 16S rRNA were amplified via PCR (ABI GeneAmp® 9700, USA), and the products were purified with AxyPrep DNA Gel Extraction Kit (AP-GX-500, Axygen Biosciences Co., Ltd., San Francisco, USA). Then, the purified products were quantified by QuantiFluor™ -ST (Promega Co., USA), and mixed in equidensity ratios. Later, the sequencing library was constructed using the TruSeqTM DNA Sample Prep Kit (FC-121−4001, Illumina, San Diego, USA) following the manufacturer's guidelines. Finally, the eligible library was sequenced via the Illumina MiSeq platform.

After subjecting samples to quality control and eliminating the non-redundant fragments, the Illumina MiSeq sequences were joined and

Table 2
Dynamic FBG in different groups (mmol/L).

	0w	1w	2w	3w	4w	5w	6w
Normal	4.60 ± 0.37	4.40 ± 0.37	4.39 ± 0.36	4.55 ± 0.44	4.53 ± 0.39	4.58 ± 0.30	5.05 ± 0.47
Model	18.96 ± 1.82**	19.01 ± 1.99**	21.16 ± 2.96**	19.68 ± 2.40**	18.21 ± 3.02**	17.10 ± 2.43**	17.47 ± 1.34**
Metformin	18.60 ± 3.64**	15.84 ± 2.52**	15.01 ± 2.48**##	9.30 ± 2.09**##	11.89 ± 3.01**##	10.4 ± 3.59**##	11.07 ± 2.12**##
BBR	18.40 ± 1.76**	14.85 ± 2.29**##	14.23 ± 1.64**##	13.68 ± 3.14**##	13.66 ± 2.90**##	12.97 ± 2.59**##	12.47 ± 2.29**##
Ab	18.90 ± 1.25**	19.51 ± 1.36**	20.71 ± 2.15**	21.12 ± 2.54**	20.48 ± 2.86**#	21.24 ± 2.17**##	21.03 ± 2.88**##
BA	18.93 ± 1.69**	18.03 ± 1.49**##	16.45 ± 1.48**##△△	15.08 ± 1.89**##△△	14.61 ± 1.25**##△△	14.60 ± 1.20**##△△	14.04 ± 2.24**##△△

Values are means ± SD, N = 7 rats for metformin group, and N = 10 rats for other groups, statistical analysis was performed using one-way ANOVA. *P < 0.05, **P < 0.01 vs. Normal; # P < 0.05, ## P < 0.01 vs. Model; △△P < 0.01 vs. Ab. BBR: berberine, Ab: antibiotics, BA: berberine+antibiotics.

NNB Exh. 2084, p. 003

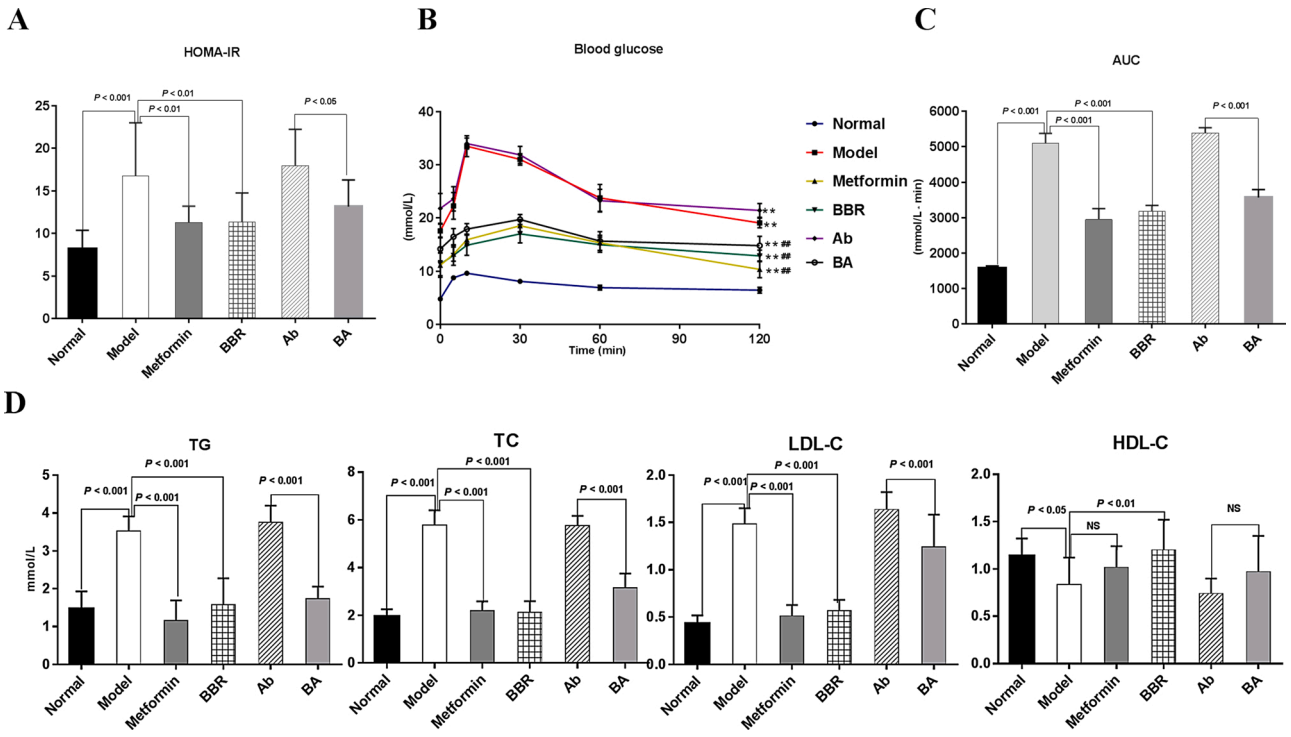


Fig. 2. Berberine (BBR) improved glucose intolerance, insulin resistance and dyslipidemia in T2DM rats. A: Homeostasis model assessment of insulin resistance index (HOMA-IR). B: Blood glucose levels of the oral glucose tolerance test (OGTT). C: Area under the curve (AUC) of the OGTT. D: Serum lipid levels. N = 7 rats for the metformin group, and N = 10 rats for other groups. Data are presented as the mean ± SD. *P < 0.05, **P < 0.01 vs. Normal; # P < 0.05, ## P < 0.01 vs. Model. Statistical analysis was performed using one-way ANOVA. NS, not significant.

mapped to the Silva 128 release database (https://www.arb-silva.de/documentation/release-128/). Using UPARSE with a 97 % similarity threshold, we selected the operational taxonomic units (OTUs). Then, the sequence numbers of the OTU were normalized using the z-score method and subject to principal coordinate analysis (PCoA) (SIMCA-P 14.1). Community richness was evaluated by the chao index and ace index, and community diversity was evaluated by the shannon index with mothur (version v.1.30.1 http://www.mothur.org/wiki/Schloss_SOP#Alpha_diversity). The heatmap of the top 20 most abundant families was portrayed using R software (pheatmap package). In addition, 16S functional prediction by PICRUSt (http://picrust.github.io/picrust) was used to analyze the metagenomic function of the gut microbiota.

2.7. Untargeted metabolomics analysis

Rats in the model group and the BBR group were selected for colon content metabolic profiling analysis.

2.7.1. Sample preprocessing

The samples of colon contents were thawed at 4 °C before analysis. 60 mg of the colon contents were added to 400 μL of water, and mixed. Then, 800 μL acetonitrile/methanol mixed solution(v:v,1:1) was added, and vortexed for 30 s. The next steps were ultrasonication (60 min) at 4 °C, twice, static placement (−20 °C, 60 min), and centrifugation (13,000 *g*, 4 °C, 15 min). Finally, the supernatant was used for the later measurements.

2.7.2. Chromatography conditions

Samples were analyzed on a 1290 UHPLC system (Agilent Technologies) with an ACQUITY UPLC BEH Amide column (1.7 μm, 2.1 mm × 100 mm, Waters, Ireland). The analysis conditions were as follows: column temperature 25 °C, flow rate 0.3 mL/min, and injection volume 2 μL. Mobile phase A was composed of deionized water +25 mM NH4OH (pH = 9.75) +25 mM ammonium acetate, whereas mobile phase B included acetonitrile. The following gradient elution procedure was performed: 0−0.5 min,95 % B; 0.5−7 min, B was linearly reduced to 65 %;7−8 min, B was linearly reduced to 40 %; 8−9 min, B was maintained at 40 %; 9–9.1 min, B was linearly increased to 95 %; and 9−12 min, B was maintained on 95 %. A random injection order was used, and quality control (QC) samples were inserted to ensure a reliable analyses.

2.7.3. Mass spectrometry conditions

After UHPLC analysis, the samples were separated, and then mass spectrum analysis was performed using an Agilent 6550 mass spectrometer. The electrospray ionization(ESI) source conditions were as follows: gas temperature, 250 °C; drying gas, 16 L/min; ebnulizer, 20 psig; sheath gas temperature, 400 °C; sheath gas flow, 12 L/min; vcap, 3000 V; nozzle voltage, 0 V; fragment, 175 V; mass range, 50–1200; acquisition rate, 4 Hz; and cycle time, 250 ms. The collected data (wiff.scan format) were saved in. mzXML format by MSconventer for further analysis.

After the samples were tested by Agilent 6550, we applied AB Triple TOF 6600 (Q-TOF, AB Sciex) to identify the metabolites, and collected the QC sample atlas. The ESI source conditions were as follows: ion source gas 1, 40; ion source gas 2, 80; curtain gas, 30; source temperature, 650 °C; ionSapary voltage floating ± 5000 V. Secondary mass spectrometry data were obtained by information dependent acquisition (IDA), and a high sensitivity model was used. The declustering potential was ±60 V. IDA conditions excluded isotopes within 4 Da, and 10 candidate ions were used to monitor each cycle. Finally, the collected data were matched with a self-built library for structural analysis.

2.7.4. Data processing

The. mzXML format data from Agilent 6550 were aligned based on peaks. Then retention time was revised, and peak area was extracted with XCMS software (version 1.41.0). Minfrac was set as 0.5. Then, these

NNB Exh. 2084, p. 004

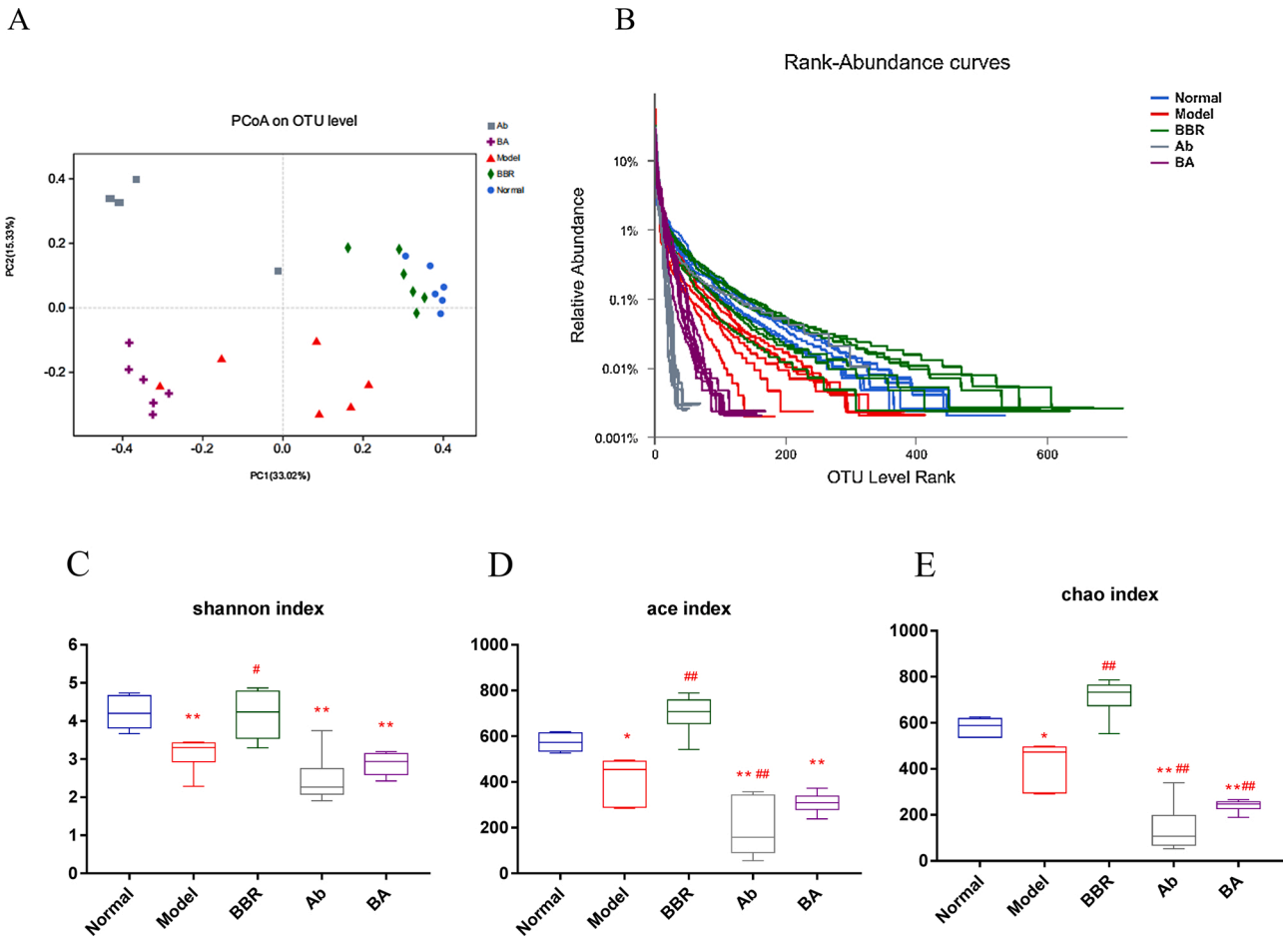


Fig. 3. Effects of BBR on gut microbiota modulation at the OTU level. A: Principal coordinate analysis (PCoA) of the microbial composition at the OTU level. B: Rank-abundance curve. C: Shannon index. D: Ace index. E: Chao index. N = 6 rats/group. Statistical analysis was performed using one-way ANOVA. $^{*}P < 0.05$, $^{**}P < 0.01$ vs. Normal; # $P < 0.05$, ## $P < 0.01$ vs. Model.

processing data were matched with the structural analysis data (obtained from AB Triple TOF 6600), and the matched parameters were *m/z* tolerance ±30 ppm and RT tolerance ± 60 s.

After the total peak area normalization with the z-score method, the processed data were imported into SIMCA-P 14.1 for multivariate data analyses. In the OPLS-DA model, the metabolites would be selected for further analysis if their variable importance in the projection (VIP) value >1 [32,35]. The normalized peak areas were subjected to Student's *t*-test (R software), and a *P* value less than 0.5 was considered statistically significant. The fold change (FC) was calculated with total peak area of the BBR group compared to the model group. Only a metabolite with VIP > 1 and *P* value<0.05, would be considered as a differential metabolite. Later, the differential metabolites were matched to the self-built library, and identified as the final differential metabolites. The heatmap of the final differential metabolites was portrayed by R software (pheatmap package), and the data were normalized with z-score method (z=(x-μ)/σ). The final differential metabolites were entered into the MetaboAnalyst (http://www.metaboanalyst.ca) for metabolic pathway analysis.

2.8. Measurement of AAAs in serum

LC/MS was used to absolutely quantify the AAAs in serum. Briefly, 50 μL serum sample was added to 400 μL acetonitrile/methanol mixed solution(v:v,1:1). The samples were sequentially vortexed 60 s, static-placed (−20 °C, 60 min), and centrifuged (14,000 *g*, 4 °C, 20 min). An agilent 1290 Infinity LC was used for UHPLC analysis and 5500 QTRAP (AB, SCIEX) was used for MS analysis. The standard curves of AAAs are provided in Table 1. The concentrations of AAAs in serum were quantified based on the standard curves and the peak areas of AAAs.

2.9. Statistical analysis

One-way ANOVA was performed to investigate alterations among three or more groups Student's t-tests were performed to compare the data between only two groups. All statistical analyses were conducted with SPSS 23.0 and expressed as the means ± SD. The figures were presented with GraphPad Prism 7.0 software. $P < 0.05$ was considered statistically significant. To observe the association between the top 20 most abundant gut microbiota and biomarkers, Spearman's correlation coefficient was established by SPSS 23.0.

3. Results

3.1. BBR attenuated symptoms in type 2 diabetic rats

Many studies have demonstrated that BBR could alleviate diabetic symptoms [6,8,15], and our study also demonstrated its therapeutic effects in type 2 diabetic rats. The dynamic FBG is listed in Table 2. Initially, FBG significantly increased in type 2 diabetic rats, indicating that the type 2 diabetic rat model was successfully established ($P < 0.01$). Compared to the model group, BBR substantially decreased the FBG from the first week ($P < 0.01$) and maintained a stable condition. FBG was also decreased in the BA group compared to the model

NNB Exh. 2084, p. 005

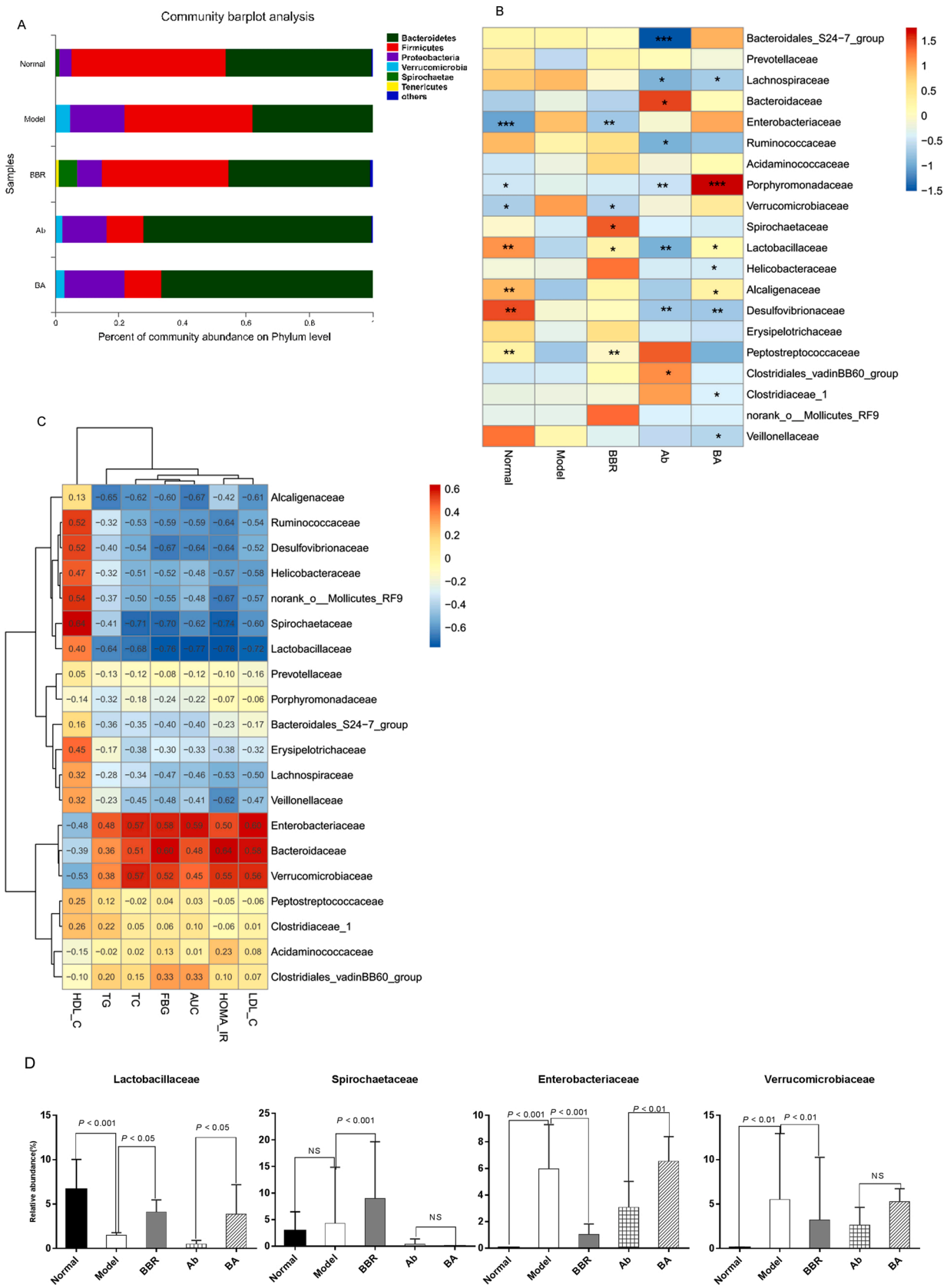


Fig. 4. Effects of BBR on gut microbiota modulation. A: Bar graph of the main gut microbiota composition at the phylum level. B: Heatmap of the top 20 most abundant families. C: Spearman's correlations of the top 20 most abundant families with biomarkers. D: Relative abundance of differential families. N=6 rats/ group. * $P < 0.05$, ** $P < 0.01$ vs Model. Statistical analysis was performed using one-way ANOVA.

NNB Exh. 2084, p. 006

Table 3
Relative abundance of phylum in different groups (%).

	Firmicutes	*Bacteroidetes*	*Proteobacteria*	*Verrucomicrobia*
Normal	48.97 ± 10.31	45.70 ± 9.94	3.71 ± 1.09	0.04 ± 0.04
Model	40.59 ± 18.15	37.46 ± 18.70	17.18 ± 8.43**	4.62 ± 4.60**
BBR	40.20 ± 12.33	44.41 ± 13.16	7.53 ± 2.97#	0.16 ± 0.25##
Ab	15.68 ± 12.90**##	64.78 ± 23.41**##	15.59 ± 8.26**	1.79 ± 1.26#
BA	11.62 ± 3.02**##	66.19 ± 4.83**##	19.20 ± 5.95**	2.92 ± 0.80*

Values are means ± SD, N = 6 rats for other groups, statistical analysis was performed using one-way ANOVA. *P < 0.05, **P < 0.01 vs. Normal; # P < 0.05, ## P < 0.01 vs. Model. BBR: berberine, Ab: antibiotics, BA: berberine + antibiotics.

group and the Ab group, but reduction was not as great as that noted in the BBR group, indicating that hypoglycemic effect of BBR is influenced by not only its own pharmacologicbut also gut microbiota. To further confirm the therapeutic effects of BBR, the HOMA-IR index and OGTT were assessed. The HOMA-IR index which reflects the insulin resistance, was decreased by 32.4 % in the BBR group ($P < 0.01$) (Fig. 2A). OGTT results confirmed that BBR could improve glucose intolerance. BBR administration in type 2 diabetic rats prevented the substantial increase in blood glucose levels in the OGTT, and the AUC was markedly decreased by 40.5 % (Fig. 2**B-C**). Similar with the results of FBG, HOMA-IR and blood glucose levels of OGTT were decreased in the BA group compared to the model and Ab groups. BBR also testified could improve dyslipidemia [9]. Compared to the model group, TG, TC and LDL-C were markedly reduced by 55.3 %, 63.3 %, and 61.6 % respectively, and HDL-C was significantly increased by 44.2 % in the BBR group (Fig. 2D). Serum lipid levels in the BA group were also improved, although the effects were less than that noted in the BBR group (Fig. 2D).

3.2. BBR increased gut microbiota community richness and diversity in type 2 diabetic rats

Because the gut microbiota is highly associated with the development of T2DM, we assessed gut microbiota composition in colon contents via the Illumina MiSeq platform. In total, 855,960 sequences were detected and 1039 OTUs were clustered (**File S1**). Beta-diversity was assessed by PCoA at the OTU level. The model, BBR, Ab and BA groups were completely distinguishable, suggesting that BBR contributed to the maintenance of a different microbial composition from them. (Fig. 3A**)**. However, the BBR and normal groups share a similar cluster, indicating that these two groups exhibit a similar gut microbiota composition. Rank-abundance curves are used to assess the diversity of gut microbiota, and the longer range of the curve on the horizontal axis represents greater diversity at the OTU level. As shown in Fig. 3B, rats in the normal and BBR groups exhibited a relative richness diversity, indicating that BBR could increase the gut microbiota diversity at the OTU level. Because antibiotics could kill the gut microorganisms, the rats in the Ab group exhibited a lowest diversity. However, this situation was improved in the BA group. To further observed community richness and diversity at the OTU level, shannon index, ace index and chao index were calculated. Rats in the BBR group exhibited a higher shannon index, ace index and chao index values, and rats in the BA group also exhibited increased richness and diversity compared with rats in the Ab group (Fig. 3 **C-E**).

3.3. BBR altered gut microbiota composition in type 2 diabetic rats

To further investigate the gut microbial composition, we described the results at the phylum level. *Bacteroidetes*, *Firmicutes*, and *Proteobacteria* were the main phyla in every group (Fig. 4A). After the antibiotics intervention, the gut microbiota composition was significantly altered. The results revealed a decrease in the relative abundance of bacteria belonging to the phylum *Firmicutes* and an increase in the relative abundance of the phylum *Bacteroidetes* in the Ab and BA groups (Table 3, Fig. 4A). The gut microbiota composition of the BBR group at the phylum level was markedly different from that in the model group, but a similar tendency was noted with the normal group. Compared to the model group, the relative abundance of *Bacteroidetes* was increased in the BBR group, and was 37.46 % in the model group, but 45.70 % in normal group and 44.41 % in the BBR group (Table 3). However, *Proteobacteria* and *Verrucomicrobia* were obviously decreased after BBR treatment. (Table 3, Fig. 4A). The relative abundance of *Proteobacteria* was 17.18 % in the model group, but only 3.71 % was in the normal group and 7.53 % in the BBR group (Table 3). In contrast to the BBR group, rats in the BA group exhibited a different gut microbiota composition at the phylum level.

Furthermore, the top 20 most abundant families were selected. Compared to the model group, families, including *Spirochaetaceae*, *Lactobacillaceae* and *Peptostreptococcaceae* were significantly increased in the BBR group ($P < 0.05$), whereas *Enterobacteriaceae* and *Verrucomicrobiaceae* are obviously decreased after BBR treatment ($P < 0.01$, Fig. 4B). To explore the associations of the gut microbiota with biomarkers, we specifically calculated the Spearman's correlation coefficient between the top 20 most abundant families and the biomarkers. *Lactobacillaceae* and *Spirochaetaceae* were strongly negatively associated with FBG, HOMA-IR, AUC, TC, TG and LDL-C, but positively associated with HDL-C (Fig. 4C). However, *Enterobacteriaceae* and *Verrucomicrobiaceae* exhibited an inverse correlation (Fig. 4C). These results indicated that *Lactobacillaceae* and *Spirochaetaceae* might be benefit for the treatment of T2DM, but *Enterobacteriaceae* and *Verrucomicrobiaceae* might be bad for the treatment of T2DM.

Lactobacillaceae, which belongs to *Firmicutes*, is commonly considered beneficial in human being's health [36], and was significantly increased not only in the BBR but also BA groups (Fig. 4D).

3.4. BBR improved energy metabolism related genes expression in gut microbiota

Furthermore, clusters of orthologous groups of proteins (COG) function analysis was performed by PICRUSt. As shown in Fig. 5 and **File S1**, we found that the energy metabolism related genes of the gut microbiome in the model group were obviously decreased. However, this tendency was reversed in the BBR group. Compared to the model group and the normal group, the gene abundance for the transport and metabolism of energy substances (including carbohydrates, amino acids and lipids) was greatly increased in the BBR group (Fig. 5B). From Fig. 5, we also know that the expression of energy metabolism related genes in the BA group was promoted compared to the model and Ab group, but the level of the increase was lower than that in the BBR group. The above results indicated that BBR alleviated the symptoms of type 2 diabetic rats possibly via the alteration of energy metabolism related genes expression in the gut microbiota.

3.5. AAAs were decreased by BBR

An untargeted metabolomics with UHPLC-QTOF/MS-based approach was used to identify the metabolites of colon contents between the model and BBR groups. In total, 11,743 peaks in positive ion mode and 5244 peaks in negative ion mode were selected for further

NNB Exh. 2084, p. 007

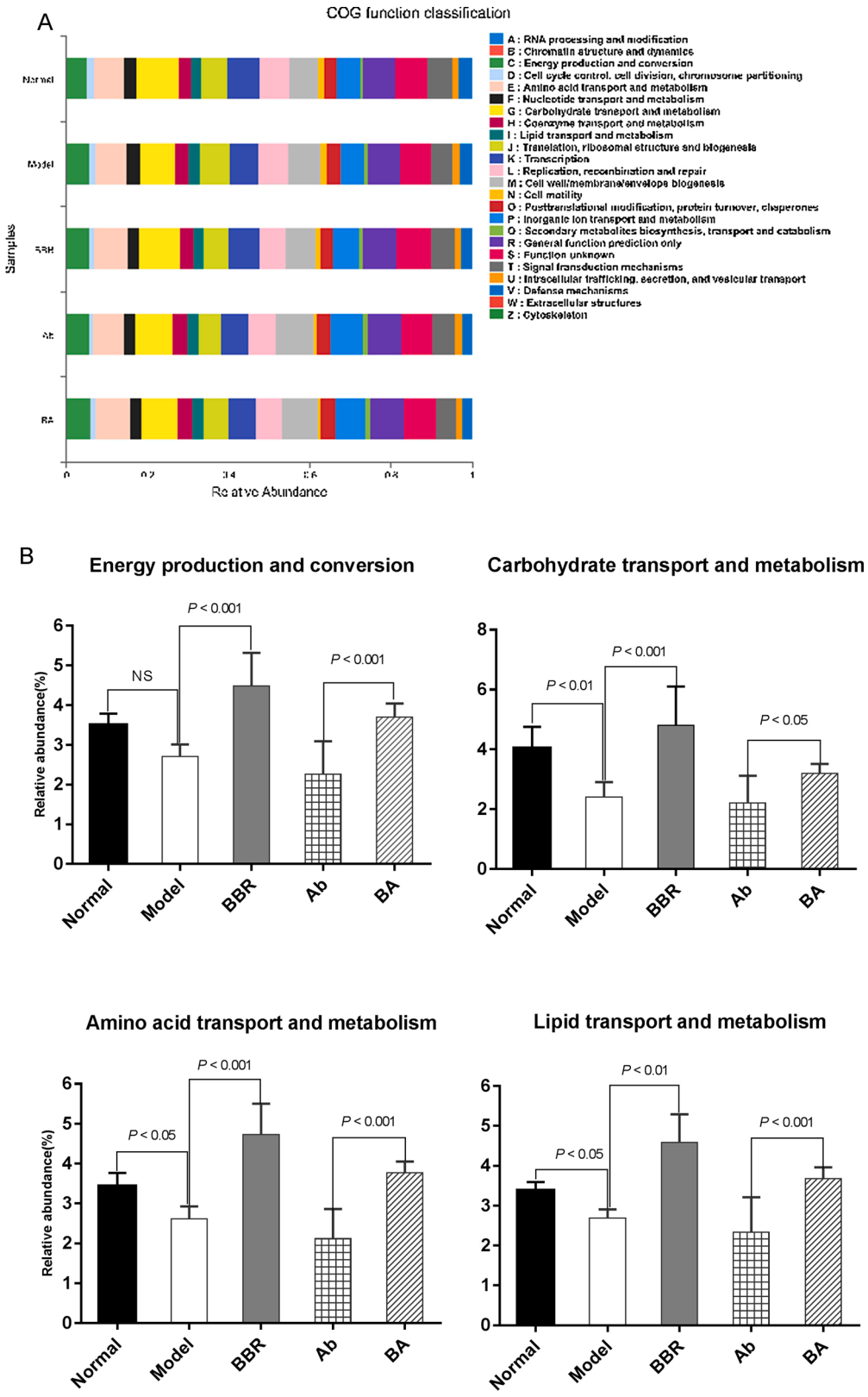


Fig. 5. Predicted gene function for the gut microbiota. A: Bar graph of COG function classifications. B: Gene abundance of COG function classifications. Statistical analysis was performed using one-way ANOVA. N = 6 rats/group.

NNB Exh. 2084, p. 008

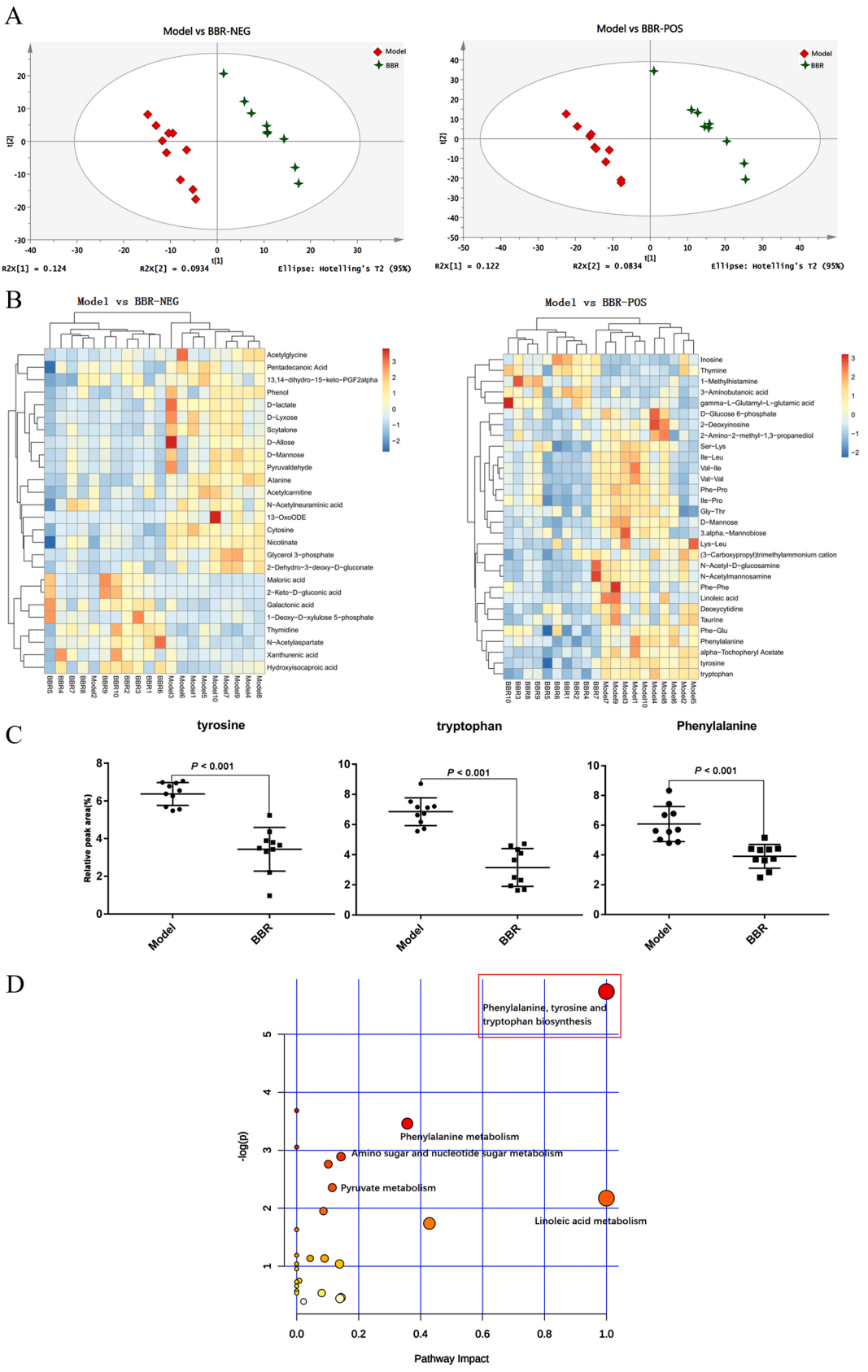


Fig. 6. Analyses of metabolites in colon contents in the model and BBR groups by UHPLC-QTOF/MS-based metabolomics. A: OPLS-DA score plots for the model and BBR groups in the positive and negative ion modes. B: Differential metabolites between the model group and the BBR group. C: Relative expression of AAAs. D: Bobble plot of pathway analysis for the differential metabolites. Statistical analysis was performed using Student's t-tests. N = 10 rats/group.

NNB Exh. 2084, p. 009

Table 4
Differential metabolites between the model and BBR groups.

Positive-ion mode				Negative-ion mode			
m/z	**rt(s)[a]**	**Metabolites**	**FC[b]**	**m/z**	**rt(s)[a]**	**Metabolites**	**FC[b]**
182.08	232.88	Tyrosine ↓[c]	0.54	130.05	281.52	Alanine ↓	0.26
176.09	415.51	Tryptophan ↓	0.46	241.08	93.96	Thymidine ↑[d]	2.08
166.08	310.99	Phenylalanine ↓	0.64	110.04	180.53	Cytosine ↓	0.45
263.14	215.59	Phe-Pro ↓	0.56	204.03	252.16	Xanthurenic acid ↑	1.42
295.12	213.11	Phe-Glu ↓	0.79	149.05	205.00	D-lactate ↓	0.43
313.15	130.10	Phe-Phe ↓	0.55	209.07	203.69	D-Lyxose ↓	0.40
177.09	300.99	Gly-Thr ↓	0.81	239.08	287.83	D-Mannose ↓	0.33
245.19	166.26	Ile-Leu ↓	0.58	359.12	287.41	D-Allose ↓	0.40
260.20	488.44	Lys-Leu ↓	0.73	202.11	264.25	Acetylcarnitine ↓	0.60
275.17	445.33	Ser-Lys ↓	0.82	152.99	253.03	Glycerol 3-phosphate ↓	0.34
229.15	222.02	Ile-Pro ↓	0.69	195.05	369.86	Galactonic acid ↑	2.20
231.17	179.71	Val-Ile ↓	0.53	174.04	73.19	N-Acetylaspartate ↑	3.09
217.15	196.14	Val-Val ↓	0.50	241.22	43.85	Pentadecanoic Acid ↓	0.66
281.25	77.66	Linoleic acid ↓	0.22	103.00	344.60	Malonic acid ↑	3.30
251.08	122.55	Inosine ↑	2.20	143.03	285.99	Pyruvaldehyde ↓	0.49
253.10	239.41	2′-Deoxyinosine ↓	0.43	122.03	197.90	Nicotinate ↓	0.71
127.05	95.73	Thymine ↓	1.81	193.03	345.16	2-Keto-D-gluconic acid ↓	3.69
228.10	277.30	Deoxycytidine ↓	0.51	93.03	161.53	Phenol ↓	0.52
490.42	31.44	alpha-Tochopheryl Acetate ↓	0.41	293.22	23.74	13-OxoODE ↓	0.13
198.10	287.01	D-Mannose ↓	0.42	131.07	123.08	Hydroxyisocaproic acid ↓	2.06
86.06	105.16	3-Aminobutanoic acid ↑	1.88	116.03	169.54	Acetylglycine ↓	0.44
125.09	33.06	1-Methylhistamine ↑	3.28	330.08	351.28	N-Acetylneuraminic acid ↓	0.74
126.02	162.78	Taurine ↓	0.58	193.05	145.12	Scytalone ↓	0.40
146.12	360.45	(3-Carboxypropyl)trimethylam-monium cation ↓	0.77	177.04	283.94	2-Dehydro-3-deoxy-D-gluconate ↓	0.57
241.08	386.37	gamma-L-Glutamyl-L-glutamic acid ↑	1.43	353.23	147.78	1314-dihydro-15-keto-PGF2α ↓	0.67
70.06	338.81	2-Amino-2-methyl-1,3-propane-diol ↓	0.63	230.05	321.03	1-Deoxy-D-xylulose 5-phosphate ↓	2.21
360.15	390.68	3α-Mannobiose ↓	0.57				
222.10	241.45	N-Acetyl-D-glucosamine ↓	0.80				
204.09	240.72	N-Acetylmannosamine ↓	0.61				
278.06	451.98	D-Glucose 6-phosphate ↓	0.60				

rt[a]: retention time. FC[b]: fold change, as determined by average peak area obtained from BBR group/model group. ↓[c]: down-regulated after BBR treatment. ↑[d]: up-regulated after BBR treatment.

Table 5
Metabolite pathway changes.

Pathway	Hits[a]	*P*	-Log (*P*)	Holm *P*[b]	FDR *P*[c]	Impact
Phenylalanine, tyrosine and tryptophan biosynthesis	3/4	0.00	5.74	0.27	0.27	1.00
Phenylalanine metabolism	2/12	0.03	3.46	1.00	0.88	0.36
Amino sugar and nucleotide sugar metabolism	3/37	0.05	2.89	1.00	0.89	0.14
Pyrimidine metabolism	3/39	0.06	2.76	1.00	0.89	0.10
Pyruvate metabolism	2/22	0.09	2.36	1.00	1.00	0.12
Linoleic acid metabolism	1/5	0.11	2.17	1.00	1.00	1.00
Taurine and hypotaurine metabolism	1/8	0.18	1.74	1.00	1.00	0.43
Starch and sucrose metabolism	1/18	0.35	1.04	1.00	1.00	0.14
Tryptophan metabolism	1/41	0.63	0.46	1.00	1.00	0.14
Tyrosine metabolism	1/42	0.64	0.44	1.00	1.00	0.14

Hits[a]: the matched number of metabolites in one pathway. Holm *P*[b]: the *P* value further adjusted using Holm-Bonferroni method. FDR *P*[c]: the *P* value adjusted using false discovery rate.

screening processes (**File S2**).

To explore the difference in metabolites between these two groups, supervised OPLS-DA patterns were introduced and revealed significant shifts in the composition of metabolites between the model group and the BBR group in not only positive but also negative ion modes, suggesting that each group had a unique metabolite profile of the colon contents (Fig. 6A).

Based on our selected threshold (VIP > 1, and $P < 0.05$), differential intestinal metabolites were matched from a self-built commercial database (**File S2**). Finally, 55 metabolites (30 in positive ion mode, 26 in negative ion model, with 1 duplicated result in both modes) were identified between the model group and the BBR group, with 47 metabolites were down-regulated and only 9 metabolites were up-regulated after BBR treatment (Fig. 6B, Table 4). Furthermore, 4 types of amino acids and 10 types of dipeptides were decreased after BBR treatment (Fig. 6B, Table 4). AAAs, including tyrosine, tryptophan and phenylalanine, were found significantly reduced in the BBR treated group ($P < 0.001$, Fig. 6C).

In light of abovementioned analysis, we resorted to a metabolic pathway analysis to reveal inner links between the matched metabolites with KEGG database. The MetaboAnalyst online database was used for metabolic pathway analysis. As shown in Fig. 6**D** and Table 5, compared to the model group, the main influential metabolic pathways (pathway impact value > 0.1, $P < 0.05$) of the BBR group were involved in phenylalanine, tyrosine and tryptophan biosynthesis, phenylalanine metabolism and amino sugar and nucleotide sugar metabolism.

To further verify the reduction in AAAs after BBR treatment, serum concentration of AAAs were detected. All three AAAs, including tyrosine, tryptophan and phenylalanine were significantly decreased in the BBR group (Fig. 7). This result was consistent with the results of untargeted metabolomics and indicated that the reduction of AAAs might be benefit for the treatment of T2DM.

4. Discussion

Our study demonstrated that BBR could restore the normal conditions in STZ induced type 2 diabetic rats. The dynamic FBG showed that BBR had a favorable effect on reducing blood glucose levels and could maintain the FBG at a steady level. HOMA-IR, OGTT and blood lipids were also improved after BBR treatment, and the ability of BBR to treat

NNB Exh. 2084, p. 010

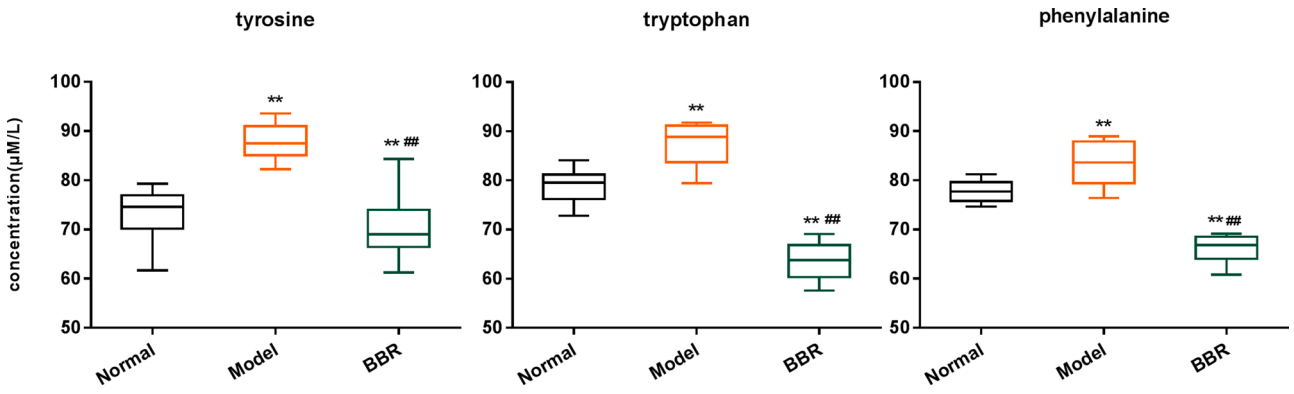


Fig. 7. Measurement of AAAs in serum. **P < 0.01 vs. Normal; ## P < 0.01 vs. Model. Statistical analysis was performed using one-way ANOVA. N = 6 rats/group.

diabetes corresponded with that reported in previous studies [8,15,37]. Type 2 diabetic symptoms in the BA group (rats treated with antibiotics and BBR) were alleviated. Given that antibiotics could wipe out most of the gut microorganisms, the therapeutic effects in the BA group are weaker compared with that noted in the BBR treatment group. These findings strongly suggested that BBR can reduce blood glucose, improve insulin sensitivity, glucose homeostasis and lipid disorders immediately, and the modulation of gut microbiota is related to the mechanism of BBR in the treatment of T2DM.

Specifically, by 16S rRNA sequencing analysis, we found that community richness and diversity analysis at the OTU level in the BBR group were increased. Numerous studies demonstrated that the richness and diversity of gut microbiota are reduced in T2DM patients, and increased them are good for the treatment of T2DM [38,39]. Some studies also found that BBR could increase the diversity of gut microbiota [40,41]. Using PCoA analysis we found that the BBR group and the BA group were significantly separated from the other groups, indicating that the gut microbiota composition was altered after the oral administration of BBR.

Describing the gut microbiota composition at the phylum level, we found that *Bacteroidetes*, *Firmicutes*, and *Proteobacteria* were the main phyla in every group, and the composition of gut microbiota was significantly altered by BBR treatment. *Bacteroidetes* was abundant in the BBR group, whereas *Proteobacteria* and *Verrucomicrobia* were increased in the model group. Because of the antibiotics intervention, the composition of the gut microbiota in the Ab and BA groups was significantly different compared with other groups and was accompanied by an increase in *Bacteroidetes* and a decrease in *Firmicute*. The normal human gut microbiota comprises of two major phyla, namely, *Bacteroidetes* and *Firmicutes* [42,43]. In our study, these two bacteria accounted for 94.81 % in the normal group, 78.07 % in the model group, and 85.06 % in the BBR group. *Firmicutes* is represented by the genera *Ruminiococcus*, *Clostridium*, and *Lactobacillus*, which is typically used as probiotics, and *Bacteroidetes* is represented by *Bacteroides, Prevotella*, and *Xylanibacter*, which has ability to degrade many complex glycans, and promote energy metabolism [44,45]. Therefore, the improvement of energy metabolism by BBR might be related to the increase in *Bacteroidetes* and *Firmicutes*. *Proteobacteria* was reported to be a common factor in human disease [46,47], and we found that the relative abundance of *Proteobacteria* was decreased by BBR. The family *Lactobacillaceae*, which belongs to the phylum *Firmicute*, is usually considered beneficial to human being's health [36,48]. Many studies have demonstrated that

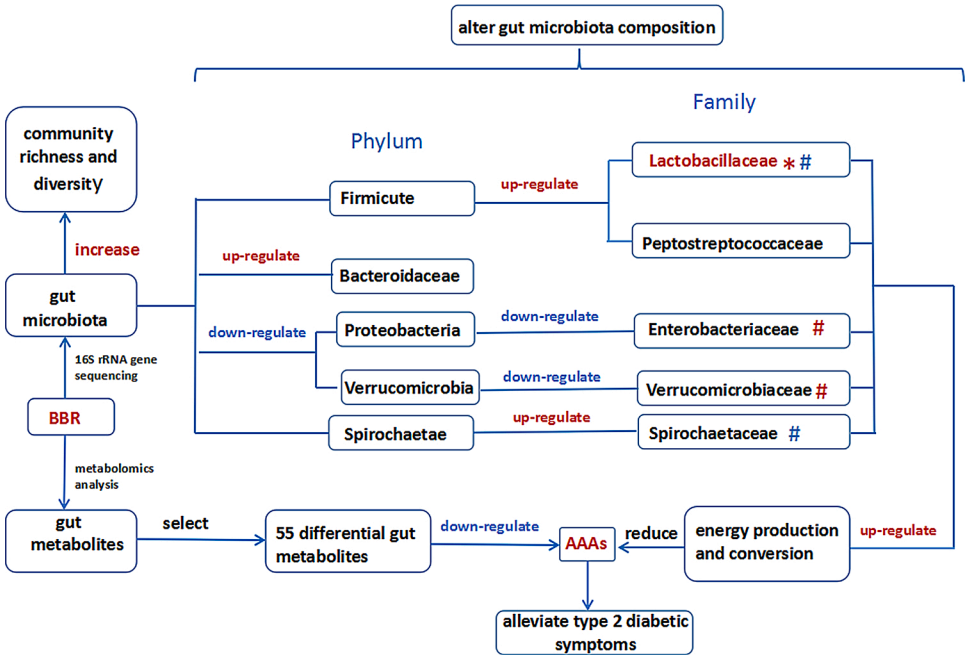


Fig. 8. The mechanism by which BBR alleviate type 2 diabetic symptoms. * indicates that this kind of bacterium was increased not only in the BBR group, but also in the BA group. Blue # indicates that this type of bacterium was negatively associated with the risk of T2DM, Red # indicates that this type of bacterium was positively associated with the risk of T2DM.

NNB Exh. 2084, p. 011

increases in the relative abundance of *Lactobacillaceae* are effective in the treatment of metabolic disorders [49,50]. In our study, *Lactobacillaceae* was increased not only in the BBR group but also in the BA group. Furthermore, Spearman's correlation analysis found that *Lactobacillaceae* was strongly negatively associated with FBG, HOMA-IR, AUC, TC, TG and LDL-C but positively associated with HDL-C, indicating that this bacterium is benefit for the treatment of type 2 diabetic rats.

COG function analysis revealed that energy metabolism (including energy production and conversion, carbohydrate transport and metabolism, amino transport and metabolism and lipid transport and metabolism) related genes of gut microbiota were obviously increased. These results suggested that after BBR treatment, the consumption of energetic substances from colon contents by gut microbiota is potentially promoted. Subsequently, the absorption of energy from the intestine by the rats might be reduced, and this change might be beneficial for treating type 2 diabetic rats.

Based on the untargeted metabolomics analysis of colon contents, we identified 55 differential intestinal metabolites between type 2 diabetic rats and the BBR treated rats, and metabolites including amino acids, dipeptides, nucleosides, fatty acids, saccharides and other metabolites, that were involved in phenylalanine, tyrosine and tryptophan biosynthesis, phenylalanine metabolism and amino sugar and nucleotide sugar metabolism. These results indicate a significant change in metabolism after BBR treatment. Furthermore, 4 types of amino acids and 10 types of dipeptides were decreased in the BBR group, and 3 AAAs, including tyrosine, tryptophan and phenylalanine, were involved in these 4 changed amino acids. In further studies, we found that the concentration of AAAs in serum also obviously decreased after BBR treatment. These changes were consistent with the notion that gut microbiota could promote amino transport and metabolism and reduce the accumulation of amino acids in the colon contents and serum, indicating that the therapeutic effects of BBR to type 2 diabetic rats might be related to the reduction of AAAs, which is mediated by gut microbiota.

AAAs are amino acids that include an aromatic ring, and phenylalanine, tryptophan and tyrosine are primary AAAs in animals. Numerous studies have revealed tight relationships between AAAs and T2DM [19,20,22,51]. Several metabolic studies have shown that AAAs are closely associated with the risk of developing T2DM. Increasing the serum levels of AAAs are accompanied with higher risk of T2DM [22,51]. GPR142 is almost exclusively expressed in endocrine cells of the gastrointestinal tract and pancreas and that functions as a highly selective receptor for AAAs, in particular tryptophan [52]. The activation of GPR142 by AAAs promoted the secretion of glucagon-like peptide-1 (GLP-1), gastric inhibitory polypeptide (GIP) and cholecystokinin (CCK), and these hormones are useful for the treatment of T2DM [52–54]. Nevertheless, studies of GPR142 were inconsistent with the serum metabolic studies of AAAs in T2DM. The effects of AAAs to T2DM need to be further determined.

In conclusion, our data provide evidences to demonstrate that BBR could alleviate symptoms in type 2 diabetic rats effectively. BBR could increase the gut microbiota community richness and diversity, and the relative abundance of *Bacteroidetes* was enhanced by BBR at the phylum level. *Lactobacillaceae*, a probiotic, was significant up-regulated after BBR treatment. COG functional analysis revealed that BBR could improve the expression of energy metabolism related genes in intestinal microorganisms, especially amino transport and metabolism related genes. Gut metabolites analyses were consistent with the above results, and AAAs in colon contents and serum were obviously decreased in the BBR group. Our study indicates that BBR alleviates type 2 diabetic symptoms might via the regulation of gut microbiota and reduction of AAAs (Fig. 8).

Authors' contributions

YY and DW conceived and designed the experiments. YY, HC, LY, and WW performed the experiments and collected the data. YY analyzed the data. YY and DW wrote the manuscript. All authors reviewed and approved the final version of the manuscript.

Declaration of Competing Interest

The authors report no declarations of interest.

Acknowledgements

This work was financially supported by Foundation of Hunan Key Laboratory of Traditional Chinese Medicine for Gan of State Administration; this research was supported by Hunan Province Science and Technology Project (No. 2016SK2008).

Appendix A. Supplementary data

Supplementary material related to this article can be found, in the online version, at doi:https://doi.org/10.1016/j.biopha.2020.110669.

References

[1] J.M. Friedman, Modern science versus the stigma of obesity, Nat. Med. 10 (2004) 563–569.
[2] M. Huang, F. Wang, X. Zhou, H. Yang, Y. Wang, Hypoglycemic and hypolipidemic properties of polysaccharides from Enterobacter cloacae Z0206 in KKAy mice, Carbohydr. Polym. 117 (2015) 91–98.
[3] N. Wang, H.Y. Tan, L. Li, M.F. Yuen, Y. Feng, Berberine and Coptidis Rhizoma as potential anticancer agents: recent updates and future perspectives, J. Ethnopharmacol. 176 (2015) 35–48.
[4] M. Imenshahidi, H. Hosseinzadeh, Berberis vulgaris and berberine: an update review, Phytother. Res. 30 (2016) 1745–1764.
[5] I.E. Allijn, B.M.S. Czarny, X. Wang, S.Y. Chong, M. Weiler, A.E. da Silva, J. M. Metselaar, C.S.P. Lam, G. Pastorin, D.P.V. de Kleijn, G. Storm, J.W. Wang, R. M. Schiffelers, Liposome encapsulated berberine treatment attenuates cardiac dysfunction after myocardial infarction, J. Control. Release 247 (2017) 127–133.
[6] C. Chen, C. Tao, Z. Liu, M. Lu, Q. Pan, L. Zheng, Q. Li, Z. Song, J. Fichna, A randomized clinical trial of berberine hydrochloride in patients with diarrhea-predominant irritable bowel syndrome, Phytother. Res. 29 (2015) 1822–1827.
[7] C.H. Lee, J.C. Chen, C.Y. Hsiang, S.L. Wu, H.C. Wu, T.Y. Ho, Berberine suppresses inflammatory agents-induced interleukin-1beta and tumor necrosis factor-alpha productions via the inhibition of IkappaB degradation in human lung cells, Pharmacol. Res. 56 (2007) 193–201.
[8] H. Zhang, J. Wei, R. Xue, J.D. Wu, W. Zhao, Z.Z. Wang, S.K. Wang, Z.X. Zhou, D. Q. Song, Y.M. Wang, H.N. Pan, W.J. Kong, J.D. Jiang, Berberine lowers blood glucose in type 2 diabetes mellitus patients through increasing insulin receptor expression, Metabolism 59 (2010) 285–292.
[9] W. Kong, J. Wei, P. Abidi, M. Lin, S. Inaba, C. Li, et al., Berberine is a novel cholesterol-lowering drug working through a unique mechanism distinct from statins, Nat. Med. 10 (2004) 1344–1351.
[10] Y.G. Ma, Y.B. Zhang, Y.G. Bai, Z.J. Dai, L. Liang, M. Liu, M.J. Xie, H.T. Guan, Berberine alleviates the cerebrovascular contractility in streptozotocin-induced diabetic rats through modulation of intracellular Ca(2)(+) handling in smooth muscle cells, Cardiovasc Diabetol.15 (2016) 63.
[11] F.H. Karlsson, V. Tremaroli, I. Nookaew, G. Bergstrom, C.J. Behre, B. Fagerberg, J. Nielsen, F. Backhed, Gut metagenome in European women with normal, impaired and diabetic glucose control, Nature. 498 (2013) 99–103.
[12] K. Forslund, F. Hildebrand, T. Nielsen, G. Falony, E. Le Chatelier, S. Sunagawa, E. Prifti, S. Vieira-Silva, V. Gudmundsdottir, H.K. Pedersen, M. Arumugam, K. Kristiansen, A.Y. Voigt, H. Vestergaard, R. Hercog, P.I. Costea, J.R. Kultima, J. Li, T. Jorgensen, F. Levenez, J. Dore, H.B. Nielsen, S. Brunak, J. Raes, T. Hansen, J. Wang, S.D. Ehrlich, P. Bork, O. Pedersen, Disentangling type 2 diabetes and metformin treatment signatures in the human gut microbiota, Nature 528 (2015) 262–266.
[13] E. Org, Y. Blum, S. Kasela, M. Mehrabian, J. Kuusisto, A.J. Kangas, P. Soininen, Z. Wang, M. Ala-Korpela, S.L. Hazen, M. Laakso, A.J. Lusis, Relationships between gut microbiota, plasma metabolites, and metabolic syndrome traits in the METSIM cohort, Genome Biol.18 (2017) 70.
[14] L. Zhao, F. Zhang, X. Ding, G. Wu, Y.Y. Lam, X. Wang, et al., Gut bacteria selectively promoted by dietary fibers alleviate type 2 diabetes, Science 359 (2018) 1151–1156.
[15] S.J. Yue, J. Liu, A.T. Wang, X.T. Meng, Z.R. Yang, C. Peng, H.S. Guan, C.Y. Wang, D. Yan, Berberine alleviates insulin resistance by reducing peripheral branched-chain amino acids, Am. J. Physiol. Endocrinol. Metab. 316 (2019) E73–e85.
[16] Y. Tian, R.G. Nichols, J. Cai, A.D. Patterson, M.T. Cantorna, Vitamin A deficiency in mice alters host and gut microbial metabolism leading to altered energy homeostasis, J. Nutr. Biochem. 54 (2018) 28–34.

NNB Exh. 2084, p. 012

[17] O. Chavez-Talavera, A. Tailleux, P. Lefebvre, B. Staels, Bile acid control of metabolism and inflammation in obesity, type 2 diabetes, dyslipidemia, and nonalcoholic fatty liver disease, Gastroenterology.152 (2017), 1679-1694.e1673.
[18] Y. Yao, L. Yan, H. Chen, N. Wu, W. Wang, D. Wang, Cyclocarya paliurus polysaccharides alleviate type 2 diabetic symptoms by modulating gut microbiota and short-chain fatty acids, Phytomedicine.77 (2020), 153268.
[19] M. Ruiz-Canela, M. Guasch-Ferre, E. Toledo, C.B. Clish, C. Razquin, L. Liang, D. D. Wang, D. Corella, R. Estruch, A. Hernaez, E. Yu, E. Gomez-Gracia, Y. Zheng, F. Aros, D. Romaguera, C. Dennis, E. Ros, J. Lapetra, L. Serra-Majem, C. Papandreou, O. Portoles, M. Fito, J. Salas-Salvado, F.B. Hu, M.A. Martinez-Gonzalez, Plasma branched chain/aromatic amino acids, enriched Mediterranean diet and risk of type 2 diabetes: case-cohort study within the PREDIMED Trial, Diabetologia 61 (2018) 1560–1571.
[20] M. Guasch-Ferre, A. Hruby, E. Toledo, C.B. Clish, M.A. Martinez-Gonzalez, J. Salas-Salvado, F.B. Hu, Metabolomics in prediabetes and diabetes: a systematic review and meta-analysis, Diabetes Care 39 (2016) 833–846.
[21] D. Preiss, N. Rankin, P. Welsh, R.R. Holman, A.J. Kangas, P. Soininen, P. Wurtz, M. Ala-Korpela, N. Sattar, Effect of metformin therapy on circulating amino acids in a randomized trial: the CAMERA study, Diabet. Med. 33 (2016) 1569–1574.
[22] T. Chen, Y. Ni, X. Ma, Y. Bao, J. Liu, F. Huang, C. Hu, G. Xie, A. Zhao, W. Jia, W. Jia, Branched-chain and aromatic amino acid profiles and diabetes risk in Chinese populations, Sci Rep.6 (2016) 20594.
[23] J. Lan, Y. Zhao, F. Dong, Z. Yan, W. Zheng, J. Fan, G. Sun, Meta-analysis of the effect and safety of berberine in the treatment of type 2 diabetes mellitus, hyperlipemia and hypertension, J. Ethnopharmacol. 161 (2015) 69–81.
[24] W. Chang, L. Chen, G.M. Hatch, Berberine as a therapy for type 2 diabetes and its complications: from mechanism of action to clinical studies, Biochem. Cell Biol. 93 (2015) 479–486.
[25] W. Chang, M. Zhang, J. Li, Z. Meng, S. Wei, H. Du, L. Chen, G.M. Hatch, Berberine improves insulin resistance in cardiomyocytes via activation of 5'-adenosine monophosphate-activated protein kinase, Metabolism 62 (2013) 1159–1167.
[26] Y. Hu, G.E. Davies, Berberine inhibits adipogenesis in high-fat diet-induced obesity mice, Fitoterapia. 81 (2010) 358–366.
[27] S.P. Gray, E. Di Marco, J. Okabe, C. Szyndralewiez, F. Heitz, A.C. Montezano, J. B. de Haan, C. Koulis, A. El-Osta, K.L. Andrews, J.P. Chin-Dusting, R.M. Touyz, K. Wingler, M.E. Cooper, H.H. Schmidt, K.A. Jandeleit-Dahm, NADPH oxidase 1 plays a key role in diabetes mellitus-accelerated atherosclerosis, Circulation 127 (2013) 1888–1902.
[28] J.Y. Zhou, S.W. Zhou, Protective effect of berberine on antioxidant enzymes and positive transcription elongation factor b expression in diabetic rat liver, Fitoterapia. 82 (2011) 184–189.
[29] W. Li, D. Li, H. Kuang, X. Feng, W. Ai, Y. Wang, S. Shi, J. Chen, R. Fan, Berberine increases glucose uptake and intracellular ROS levels by promoting Sirtuin 3 ubiquitination, Biomed. Pharmacother. 121 (2020), 109563.
[30] C.S. Liu, Y.R. Zheng, Y.F. Zhang, X.Y. Long, Research progress on berberine with a special focus on its oral bioavailability, Fitoterapia. 109 (2016) 274–282.
[31] S. Gheibi, K. Kashfi, A. Ghasemi, A. Practical guide for induction of type-2 diabetes in rat: incorporating a high-fat diet and streptozotocin, Biomed. Pharmacother. 95 (2017) 605–613.
[32] W. Wang, L. Zhao, Z. He, N. Wu, Q. Li, X. Qiu, L. Zhou, D. Wang, Metabolomics-based evidence of the hypoglycemic effect of Ge-Gen-Jiao-Tai-Wan in type 2 diabetic rats via UHPLC-QTOF/MS analysis, J. Ethnopharmacol. 219 (2018) 299–318.
[33] D. Liu, Y. Zhang, Y. Liu, L. Hou, S. Li, H. Tian, T. Zhao, Berberine modulates gut microbiota and reduces insulin resistance via the TLR4 signaling pathway, Exp. Clin. Endocrinol. Diabetes 126 (2018) 513–520.
[34] T.R. Wu, C.S. Lin, C.J. Chang, T.L. Lin, J. Martel, Y.F. Ko, D.M. Ojcius, C.C. Lu, J. D. Young, H.C. Lai, Gut commensal Parabacteroides goldsteinii plays a predominant role in the anti-obesity effects of polysaccharides isolated from Hirsutella sinensis, Gut. 68 (2019) 248–262.
[35] Y. Zhao, S. Nie, M. Yi, N. Wu, W. Wang, Z. Zhang, Y. Yao, D. Wang, UPLC-QTOF/MS-based metabolomics analysis of plasma reveals an effect of Xue-Fu-Zhu-Yu capsules on blood-stasis syndrome in CHD rats, J Ethnopharmacol.241 (2019), 111908.
[36] D.D. Heeney, M.G. Gareau, M.L. Marco, Intestinal Lactobacillus in health and disease, a driver or just along for the ride? Curr. Opin. Biotechnol. 49 (2018) 140–147.
[37] Y. Dong, Y.T. Chen, Y.X. Yang, X.J. Zhou, S.J. Dai, J.F. Tong, D. Shou, C. Li, Metabolomics study of type 2 diabetes mellitus and the AntiDiabetic effect of Berberine in zucker diabetic fatty rats using Uplc-ESI-Hdms, Phytother. Res. 30 (2016) 823–828.
[38] J. Qin, Y. Li, Z. Cai, S. Li, J. Zhu, F. Zhang, et al., A metagenome-wide association study of gut microbiota in type 2 diabetes, Nature 490 (2012) 55–60.
[39] K.E. Bouter, D.H. van Raalte, A.K. Groen, M. Nieuwdorp, Role of the gut microbiome in the pathogenesis of obesity and obesity-related metabolic dysfunction, Gastroenterology 152 (2017) 1671–1678.
[40] H. Pan, Z. Li, J. Xie, D. Liu, H. Wang, D. Yu, Q. Zhang, Z. Hu, C. Shi, Berberine influences blood glucose via modulating the gut microbiome in grass carp, Front Microbiol.10 (2019) 1066.
[41] W. Zhang, J.H. Xu, T. Yu, Q.K. Chen, Effects of berberine and metformin on intestinal inflammation and gut microbiome composition in db/db mice, Biomed Pharmacother.118 (2019), 109131.
[42] S.M. Jandhyala, R. Talukdar, C. Subramanyam, H. Vuyyuru, M. Sasikala, D. Nageshwar Reddy, Role of the normal gut microbiota, World J. Gastroenterol. 21 (2015) 8787–8803.
[43] R.E. Ley, P.J. Turnbaugh, S. Klein, J.I. Gordon, Microbial ecology: human gut microbes associated with obesity, Nature. 444 (2006) 1022–1023.
[44] G.M. Barlow, A. Yu, R. Mathur, Role of the gut microbiome in obesity and diabetes mellitus, Nutr. Clin. Pract. 30 (2015) 787–797.
[45] P. Lapebie, V. Lombard, E. Drula, N. Terrapon, B. Henrissat, Bacteroidetes use thousands of enzyme combinations to break down glycans, Nat Commun.10 (2019) 2043.
[46] G. Rizzatti, L.R. Lopetuso, G. Gibiino, C. Binda, A. Gasbarrini, Proteobacteria: a common factor in human diseases, Biomed Res Int.2017 (2017), 9351507.
[47] A. Rodriguez-Palacios, F. Cominelli, Myeloperoxidases and Proteobacteria: reliable interspecies biomarkers to identify and monitor pro-inflammatory diets in humans, Inflamm. Bowel Dis. 25 (2019) e1–e2.
[48] P. Vitellio, G. Celano, L. Bonfrate, M. Gobbetti, P. Portincasa, M. De Angelis, Effects of Bifidobacterium longum and Lactobacillus rhamnosus on gut microbiota in patients with lactose intolerance and persisting functional gastrointestinal symptoms: a randomised, double-blind, cross-over study, Nutrients.11 (2019).
[49] O. BA, O. H. C, W. L, E.-R. GD, R. JW, C. W, L. D, S. BJ, L. EA, Wheat germ supplementation increases Lactobacillaceae and promotes an anti-inflammatory gut milieu in C57BL/6 mice fed a high-fat, high-sucrose diet, J. Nutr. 149 (2019) 1107–1115.
[50] L. L, Y. Y, L. Y, Q. J, L. X, Z. G, A comprehensive genome survey provides novel insights into bile salt hydrolase (BSH) in Lactobacillaceae, Molecules 23 (2018).
[51] T.J. Wang, M.G. Larson, R.S. Vasan, S. Cheng, E.P. Rhee, E. McCabe, G.D. Lewis, C. S. Fox, P.F. Jacques, C. Fernandez, C.J. O'Donnell, S.A. Carr, V.K. Mootha, J. C. Florez, A. Souza, O. Melander, C.B. Clish, R.E. Gerszten, Metabolite profiles and the risk of developing diabetes, Nat. Med. 17 (2011) 448–453.
[52] O. Rudenko, J. Shang, A. Munk, J.P. Ekberg, N. Petersen, M.S. Engelstoft, K. L. Egerod, S.A. Hjorth, M. Wu, Y. Feng, Y.P. Zhou, J. Mokrosinski, P. Thams, F. Reimann, F. Gribble, J.F. Rehfeld, J.J. Holst, J.T. Treebak, A.D. Howard, T. W. Schwartz, The aromatic amino acid sensor GPR142 controls metabolism through balanced regulation of pancreatic and gut hormones, Mol. Metab. 19 (2019) 49–64.
[53] H.V. Lin, A.M. Efanov, X. Fang, L.S. Beavers, X. Wang, J. Wang, I.C. Gonzalez Valcarcel, T. Ma, GPR142 controls tryptophan-induced insulin and incretin hormone secretion to improve glucose metabolism, PLoS One 11 (2016), e0157298.
[54] Y. Ueda, H. Iwakura, M. Bando, A. Doi, H. Ariyasu, H. Inaba, S. Morita, T. Akamizu, Differential role of GPR142 in tryptophan-mediated enhancement of insulin secretion in obese and lean mice, PLoS One.13 (2018), e0198762.

NNB Exh. 2084, p. 013